Negative-differential-resistance effects in the $TlGaTe_2$ ternary semiconductor

M. P. Hanias and A. N. Anagnostopoulos
Department of Physics, Solid State Section 313-1, Aristotle University of Thessaloniki, 54006 Thessaloniki, Greece
(Received 23 July 1991; revised manuscript received 9 October 1992)

I-U characteristics measured in $TlGaTe_2$ single crystals consist of two regimes: a linear one at low current densities and a nonlinear one at higher current densities. In the nonlinear part [negative-differential-resistance (NDR) region] of the curves, a considerable increase of the temperature of the sample was registered. Additionally, voltage oscillations were observed in this region. Arrhenius plots ($\ln\sigma$ vs $10^3/T_0$ plots) recorded in the Ohmic part of the *I-U* curves show a temperature dependence of the conductivity. This fact, in combination with a purely thermal mechanism, can well explain both the formation of the NDR region and the temperature elevation in this region.

I. INTRODUCTION

During recent years much attention has been paid to systems that behave in certain respects as if they had less than three spatial dimensions. Such materials are often called quasi-one-dimensional solids or linear-chain materials.

The $Tl(In,Ga)X_2$ (X = S, Se, Te) family belongs to these types of materials, in which the one-dimensional organization of the $[In^{3+}X^{2-}]$ chains along the c axis shapes its electronic properties.[1,2] The electrical, optical, and structural properties of these materials are all of interest, but we shall mainly discuss the electrical conductivity and shall try to elucidate the conduction mechanism of the family member $TlGaTe_2$.

The presence of an *S*-type *I-U* characteristic in two members of the family[1,2] has already been confirmed, and a further investigation of the electrical properties of $TlGaTe_2$ will be necessary. This aim is supported by the fact that there are fewer references concerning *S*-type characteristics and switching effects connected with an electrothermal mechanism in single crystals than about amorphous chalcogenide glass systems. The switching itself could play an important role in technological applications (switching and memory devices, thermistors). In addition, voltage oscillations appearing in the negative-differential-resistance (NDR) region give evidence of a chaotic system that might be useful for phase-space analysis.

$TlGaTe_2$ single crystals were grown by the direct melting of pure stoichiometric amounts of their constituent elements. The crystals were obtained after a slow cooling down to room temperature. From Debye powder patterns the lattice parameters $a = 8.316$ A and $c = 6.844$ A were obtained in quite good agreement with those reported in the literature.[3]

II. ELECTRICAL MEASUREMENTS

$TlGaTe_2$ samples used for electrical measurements were cleaved from larger crystals grown in the same ampoules as those used for the structural investigations. They were rectangularly shaped with parallel faces and dimensions of the order $7\times1\times1$ mm^3. In, Au, and Ag were found to form Ohmic contacts of low resistance with $TlGaTe_2$. This was proved by the four-point method, by successive resistivity measurements on samples of different thicknesses, as well as by photoconductivity measurements. In a recent paper,[4] it has also been reported that Ag forms Ohmic contacts with this compound. In the present work, evaporated In stripes were used as contacts to perform the electrical measurements in $TlGaTe_2$. The current-providing contacts were applied on the ends of the rectangular samples and oriented so that the current flowed along the c axis of the material. Two kinds of measurements were carried out on $TlGaTe_2$, current-voltage characteristics (*I-U* curves) and Arrhenius plots ($\ln p$ vs $10^3/T_0$ curves). It has to be mentioned here that all samples in the present report were *p*-type, as this was estimated by thermal electromotive force (emf) measurements.

A. *I-U* curves

A current source was used for this purpose [as is usual in current-controlled negative-differential-resistance (CC-NDR) regions], and the voltage drop was registered as a function of the current. Current-voltage characteristics were measured at different ambient temperatures T_0 in the range 340–60 K (Figs. 1 and 2). At low applied voltages, the measured *I-U* curves showed an Ohmic behavior. At higher currents the *I-U* characteristics turned out to be strongly nonlinear and S shaped. In the Ohmic region of the *I-U* curves, the sample retained the ambient temperature T_0, while in the NDR region the temperature of the sample was increased at a temperature T, generally higher than the ambient one. As is observed in the curves of Figs. 1 and 2 they show some common features, such as the following.

S-shaped curves in the higher current regions with a rather pronounced negative-differential-resistance region, which sets in after a critical current value I_{th} (threshold current).

The NDR portions of the curves are more pronounced at lower ambient temperatures.

The transition from the low- to the high-conductivity

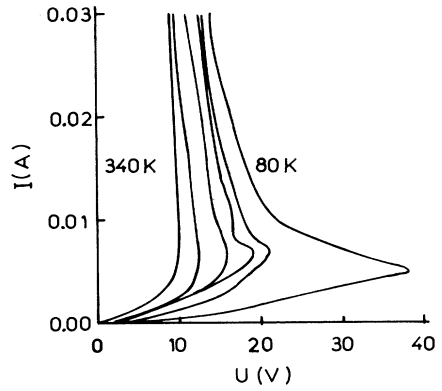

FIG. 1. Current-voltage (I-U) characteristics measured at different temperatures in $TlGaTe_2$. The Ohmic and NDR regions are apparent in these curves.

state of the curves is almost abrupt at lower temperatures.

The threshold voltage V_{th}, after which the NDR region sets in, becomes higher with decreasing temperature. In addition, voltage oscillations were observed in the NDR regions. Some of these oscillations seem to be rather periodic, while most of them are of a rather chaotic nature, both in their amplitude and in their repetition rate.

B. Arrhenius plots

In the Ohmic region of each I-U characteristic, the conductivity σ was estimated. Provided that the mobility and its temperature dependence are known,[5] the free-hole concentration p can be deduced. The corresponding $\log_{10}p$ vs $10^3/T_0$ curve is given in Fig. 3. The electrical neutrality equation in the present case gives[2,6]

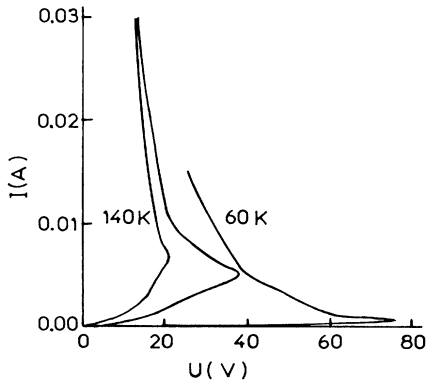

FIG. 2. Current-voltage (I-U) characteristics measured at different temperatures in $TlGaTe_2$. The Ohmic and NDR regions are apparent in these curves. Comparison of the curves of this figure with those of the previous one shows that the NDR region becomes more pronounced at lower ambient temperatures.

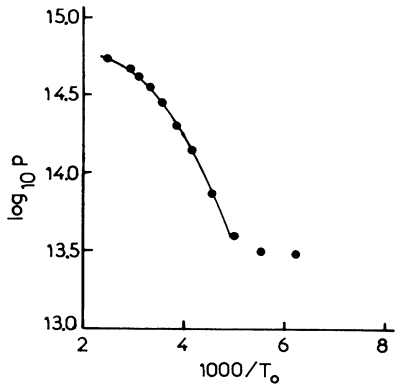

FIG. 3. The $\log_{10}p$ vs $10^3/T_0$ plot for $TlGaTe_2$, as measured in the Ohmic region of the corresponding I-U characteristics (solid circles) and as calculated using Eq. (1) with the following parameters: $E_A-E_v=0.22$ eV, $A=7\times10^{14}$ cm^{-3}, $C=3.3\times10^{14}$ cm^{-3} (solid line).

$$10^3/T_0=-\frac{10^3k_B}{E_A-E_v}[\ln p+\ln(p+C)-\ln(A-C-p)-\ln N_v]\ , \quad (1)$$

where E_v is the upper valence-band edge, E_A is the energy position of the considered acceptor level, N_v is the effective density of states in the valence band, C is the total concentration of compensating donors, and A is the concentration of the considered acceptor level.

A differential evaluation of Eq. (1) leads to the following expression for the slope $d\ln p/d(10^3/T_0)$ of the $\log_{10}p$ vs $10^3/T_0$ plot:[6]

$$\frac{d\ln p}{d(10^3/T_0)}=-\frac{(E_A-E_v)}{10^3k_B}\left[1+\frac{Ap}{(p+C)(A-C-p)}\right]^{-1}. \quad (2)$$

Depending on the degree of compensation ($C=0$, $0<C<A$, $C\rightarrow A$), the above equation can be reduced to more simple forms.

The measured $\log_{10}p$ vs $10^3/T_0$ curve (circles in Fig. 3) was fitted with cubic splines and subsequently its slope was calculated as a function of $\log_{10}p$ (Fig. 4). This curve consists of two linear parts, I and II. Part I corresponds to the temperature region where $p<C<A$, and part II corresponds to the region where $C<p<A$. From the horizontal part I, the energy level E_A of the acceptor can be obtained, while from the intersection of part II with the x axis the concentration A of this level can be deduced. The compensation C corresponds to point D (Fig. 4) with the coordinates $[C,\frac{2}{3}(E_A-E_v)]$. In the present case the following results were obtained: $E_A-E_v=0.22$ eV, $A\approx7\times10^{14}$ cm^{-3}, and $C\approx3.3\times10^{14}$ cm^{-3}. Nagat, Gamal, and Hussein[4] have also found an acceptor level at 0.21 eV above the valence band of $TlGaTe_2$. With these values we tried to fit the measured $\log_{10}p$ vs $10^3/T_0$ characteristic with the help of Eq. (1).

The result is presented in Fig. 3 by the solid line; it

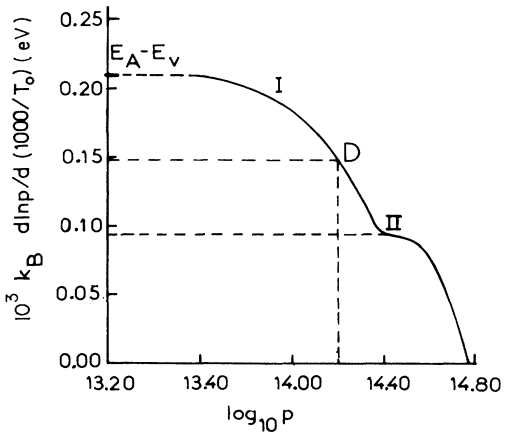

FIG. 4. The $d\ln p/d(10^3/T_0)$ vs $\log_{10}p$ plot for $TlGaTe_2$ as deduced from the corresponding experimental curve of Fig. 3 after this curve was fitted with cubic splines. Note that the horizontal part of the $d\ln p/d(10^3/T_0)$ vs $\log_{10}p$ plot corresponds to the energy level $E_A - E_v = 0.22$ eV.

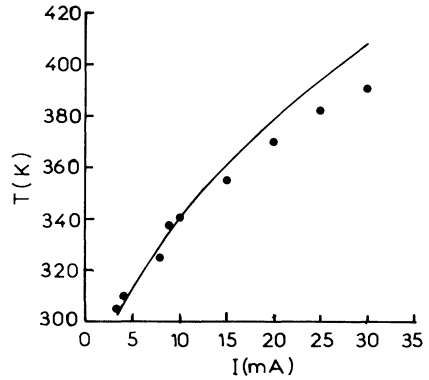

FIG. 6. The elevated sample temperature T vs the current I flowing through it in $TlGaTe_2$ as measured in the sample (solid circles) and as computed using Eqs. (2) of Ref. 7 with $E_A - E_v = 0.22$ eV (solid line).

should be mentioned here that the experimental Arrhenius plot of Fig. 3 shows a second horizontal part in the low-temperature region, which denotes the existence of a second acceptor level lying closer to the valence band than the first one, but the measurements do not allow an estimation of its level and concentration.

C. CC-NDR region

In the NDR region of the I-U curve we measured the sample temperature T at every point of it by means of a thermoelement applied on the sample. A heat-conducting and electrically insulating paste was used for this purpose. These results are shown in Fig. 5. The measurements reveal that the sample temperature was higher than that of the ambient temperature T_0. In Fig. 6 the elevated sample temperature T is presented as a function of the current flowing through it. Figure 7 shows the threshold voltage V_{th} plotted as a function of the ambient temperature T_0. Some of the voltage oscillations registered in the NDR regions of the corresponding I-U curves are shown in Figs. 8(a) and 8(b).

As is apparent from Figs. 5 and 6 the current-controlled (CC-NDR) region is correlated with an increase of the temperature of the sample. Furthermore, according to Figs. 1, 2, and 7 there is a migration of the threshold voltage to higher values with decreasing ambient temperature and a weaker appearance of the NDR region of the I-U characteristic as the ambient temperature increases.

These facts give evidence of an electrothermal process that is responsible for the appearance of the NDR region.[8] In electrothermal processes it is assumed that small local deviations from the homogeneous distribution of the imperfections lead to a higher current density in these regions. Such elevated current densities are usually accompanied by the formation of high-current-density filaments in the sample. In this "channel" the elevated current density results in an increased power dissipation, leading to Joule heating. As the temperature increases, conductivity also increases, permitting a higher current to pass through. The steady state of this path is reached when the heat dissipation equals heat losses.

In order to prove that our experimental results can also

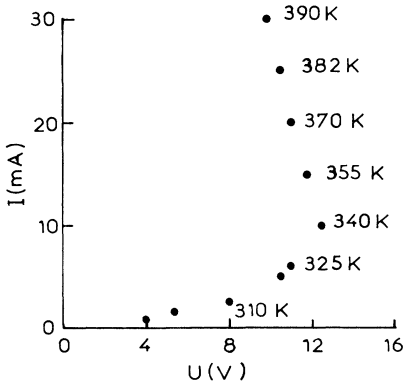

FIG. 5. The temperature evaluations as estimated in the NDR region of the I-U curve (300 K) in $TlGaTe_2$.

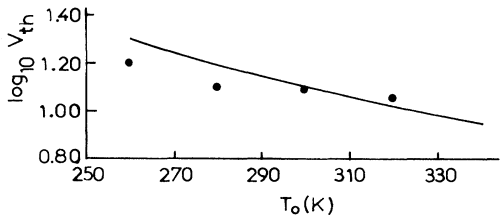

FIG. 7. The dependence of the threshold voltage V_{th} on the ambient temperature T_0 in the case of $TlGaTe_2$; measurements are denoted by solid circles while the solid line represents calculations with relation (6).

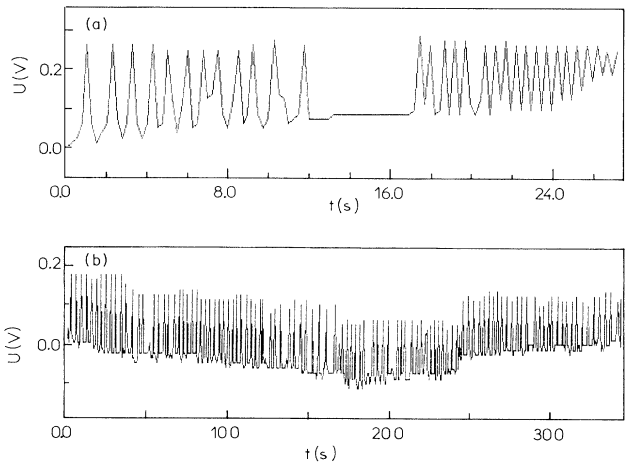

FIG. 8. (a) and (b) Observed voltage oscillations at two different samples at $T_0=300$ K, as recorded in the NDR region of the related $I(U)$ curves, immediately after I_{th} and far away from I_{th}, correspondingly.

be described quantitatively by an electrothermal process we suppose in a first approximation that the filament fills the whole sample. This model was applied in the cases of $TlInX_2$ ($X=$Se, Te) with satisfactory results.[2] According to Ref. 8, the steady state at every point of the NDR region is governed by the following relations:

$$-\frac{8\kappa}{d^2}(T-T_0)+\sigma(T,E)E^2=0 \ , \tag{3}$$

$$I=S\sigma(T,E)E \ , \tag{4}$$

and

$$U=Ed \ , \tag{5}$$

where κ is the thermal conductivity coefficient, d is the distance between the electrodes, E is the electric-field strength, I is the current, U is the voltage drop, S is the cross section of the sample, and σ its specific conductivity.

The sample temperature T is measured at every point of the I-U characteristic; so, using Eqs. (3)–(5) the generation of the corresponding characteristics was carried out. In Fig. 9 a typical example is given. Measured points are denoted by circles, while solid lines represent solutions from Eqs. (3)–(5).

The threshold voltage V_{th}, as indicated in the literature, strongly depends on the ambient temperature. In the case where the distance d between the electrodes is large, compared with the other sample dimensions, the following relation holds:[8]

$$V_{th}\rightarrow d\left[\frac{8k_B\kappa}{\sigma_0(E_A-E_v)}\right]^{1/2} T_0\exp[(E_A-E_v)/2k_BT_0] \ , \quad d\rightarrow\infty \tag{6}$$

where σ_0 is the prefactor of the thermally activated conductivity $\sigma=\sigma_0\exp[(E_A-E_v)/k_BT_0]$. For our $TlGaTe_2$ samples d was ~ 0.7 cm. In Fig. 7 the measured V_{th} values (circles) are plotted versus the ambient temperature T_0. The solid line represents the corresponding curve, as predicted from Eq. (6).

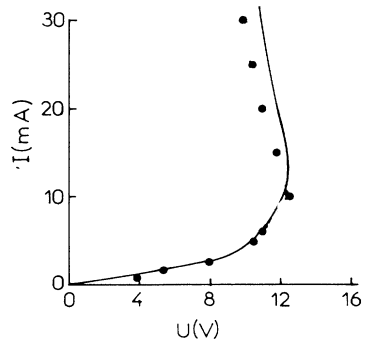

FIG. 9. The I-U curve as measured at 300 K in $TlGaTe_2$ (solid circles) and as recreated with the help of Eqs. (3)–(5) (the solid line).

D. Oscillations

Voltage oscillations have been observed in the NDR regions, as has been frequently reported in the literature.[1,2,9,10] Precursor voltage pulses also occur just below the threshold current I_{th}. Depending on temperature and on the fixed current values for which the oscillations were registered, these oscillations were of different "frequency." Figures 8(a) and 8(b) show voltage oscillations appearing in $TlGaTe_2$ at 300 K for two different samples in the NDR region of the corresponding I-U curves. The signal of Fig. 8(a) was registered in the NDR region immediately after exceeding I_{th}, while the signal of Fig. 8(b) was registered in the NDR region far away from I_{th}. A mean repetition rate of the oscillations in the range of some hertz was determined. In Figs. 10(a) and 10(b), the

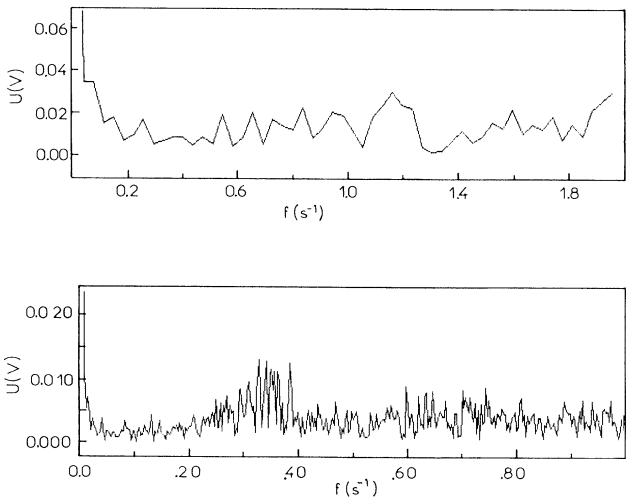

FIG. 10. (a) and (b) The corresponding power spectra of Figs. 8(a) and 8(b).

corresponding power spectra of these oscillations are presented. As is evident from these spectra no definite frequency appears in these oscillations, and their behavior could be characterized by phase portraits, which are presented in Figs. 11(a) and 11(b). Both of them present some common features, such as trajectories restricted in a limited area of the phase plane and trajectories obtained with different initial conditions that are rapidly converging in the area covered by the long life terms of the oscillations. All these facts suggest that the oscillatory behavior of the $TlGaTe_2$ in its NDR region is determined by a chaotic attractor.

In order to study the chaotic state we apply the method introduced by Grassberger and Procaccia.[11–13] This method was already used successfully in similar cases.[14] Following Refs. 11 and 12 we calculated the correlation integral, for the measured voltage signal, defined by the following relation:

$$C_m(l)=\lim_{N\to\infty}\frac{1}{N^2}\sum_{i,j=1}^{N}\Theta\left[l-\left[\sum_{k=1}^{m}|X_{i+k}-X_{j+k}|^2\right]^{1/2}\right]. \tag{7}$$

In this definition N is the number of points and Θ is the Heaviside function. The vector $X_i=\{U(t_i), U(t_i+\tau), U(t_i+2\tau), \ldots, U(t_i+(m-1)\tau)\}$ represents a point of the m-dimensional phase space in which the attractor is embedded each time. Dividing this space into hypercubes with a linear dimension l we count all points with mutual distances less than l. It has been proven[11–14] that, if our attractor is a strange one, the correlation integral is proportional to l^{ν}, where ν is a measure for the dimension of the attractor called the correlation exponent.

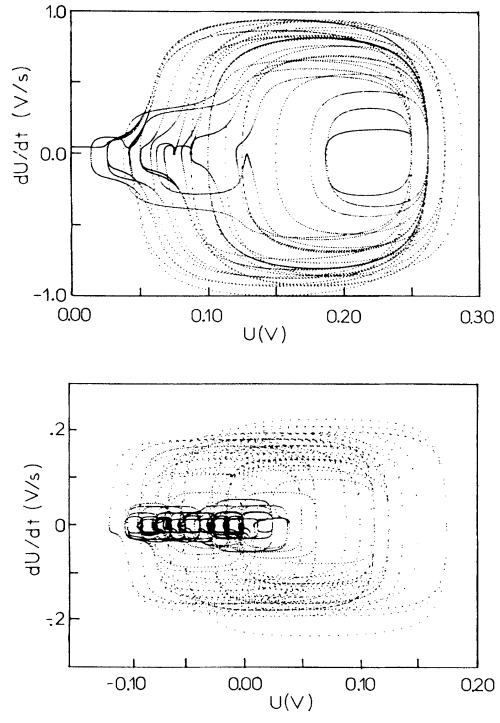

FIG. 11. (a) and (b) The corresponding phase diagrams of the voltage oscillations of Figs. 8(a) and 8(b).

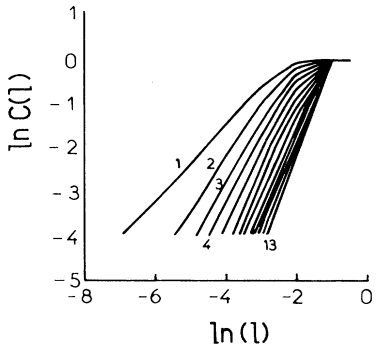

FIG. 12. The correlation function $C(l)$ vs the hypercube edge length l as calculated from the experimental data of Fig. 8(b) for different values of the embedding dimension m.

From our measured signals and using Eq. (7) we have calculated $C(l)$ as a function of l for different embedding dimensions m. These results are presented in Fig. 12. The curves of this figure show that $C(l)$ is indeed proportional to l^{ν}, as long as the hypercubes are not of the same order of magnitude with the space filled by the attractor. The slopes of the linear parts of the curves in Fig. 12 are shown in Fig. 13 as a function of m. For low values of m, ν increases proportionally to it, but at higher values of m, ν tends asympotically to the positive finite value of 2.1. This fact excludes the case of stochastic oscillations, since in the latter case ν would increase proportionally to m for all values of m.

In order to get a more precise measure of the strength of the chaos present in the voltage oscillations we have introduced the Kolmogorov entropy. According to Refs. 11–14 the method described above also gives an estimate of the Kolmogorov entropy, i.e., the correlation integral $C(l)$ scales with the embedding dimension m according to the following relation:

$$C(l)\sim e^{-m\tau K_2}, \tag{8}$$

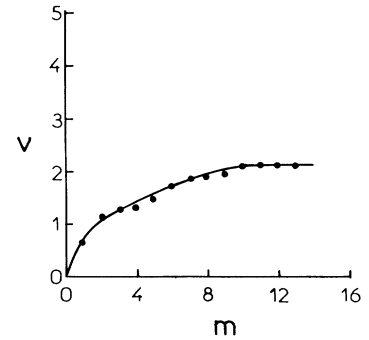

FIG. 13. The correlation exponent ν as a function of the embedding dimension m.

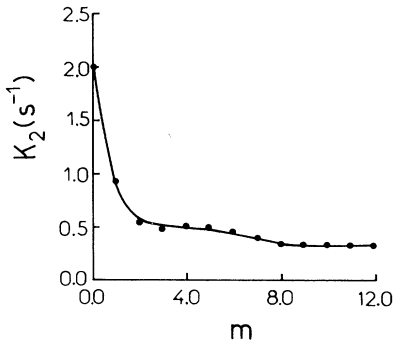

FIG. 14. The entropy parameter K_2 as calculated from the data of Fig. 12.

where K_2 is a lower bound to the Kolmogorov entropy. In Fig. 14 the average values of K_2, as deduced using the relation[14]

$$K_{2,m}(l)=\frac{1}{\tau}\ln\frac{C_m(l)}{C_{m+1}(l)} \tag{9}$$

and the corresponding data of Fig. 12, are plotted versus m. With increasing m, K_2 tends to the positive finite value $\sim 0.35\ s^{-1}$. This value is in agreement with the assumption that the observed voltage oscillations are determined by a chaotic attractor, since in the other two possible cases the Kolmogorov entropy is either 0 (ordered systems) or infinite (stochastic systems).

III. CONCLUSIONS

(a) The experimental I-U characteristics of $TlGaTe_2$ single crystals are linear for low current densities and nonlinear for high current densities. The nonlinear regimes (NDR regions) are of the S type. In these regions voltage oscillations appear, which seem to be of a chaotic nature.

(b) The steady-state I-U characteristics and especially their NDR regions can be interpreted, in a first approximation, by an electrothermal mechanism. At low current values this fitting is satisfactory, but at currents higher than the threshold, deviations, exceeding in some cases 50%, between measurements and theory can be observed, in Fig. 9.

This discrepancy can be explained if we take into account that for the generation of the I-U characteristic of Fig. 9, using Eqs. (3)–(5), the precise determination of the temperature of the sample is required. But at high current values (exactly where the deviations appear) it is plausible to expect that the heating of the sample is lower on its surface, from which a heat uptake is much easier than from its volume. This may lead to lower temperature indications of the thermoelements used to monitor the temperature of the sample.

On the other hand, an increased heating of the inner part of the specimen causes an elevation of the free-carrier concentration in this region because of the semiconducting character of $TlGaTe_2$. A high conductivity filament can thus be created in the interior of the sample. Current filamentation is already mentioned in the literature[15,16] in similar cases. Hence, a precise fitting of the I-U curves requires not only the determination of the surface temperature, but also the determination of the temperature and the free-carrier concentration in the interior of the crystal.

(c) It has to be mentioned that signals registered in the NDR regions of the I-U curves, immediately after I_{th} is exceeded, show chaotic behavior, which is interrupted by flat parts, Fig. 8(a). On the other hand, oscillations registered in the NDR regions of the corresponding I-U curves far away from I_{th} show a well-developed chaotical behavior, not interrupted by flat parts, Fig. 8(b). A detailed study of the correlation between the frequency of the occurrence and the length of such flat parts with the distance from I_{th} is still in progress, but preliminary results strongly suggest that the route to chaos of the $TlGaTe_2$ single crystals is of the intermittency type. In such a case, flat parts between chaotic bursts represent the corresponding laminar lengths. For these reasons only the signal of Fig. 8(b) was analyzed by the Grassberger-Procaccia method.

(d) Long-term drifts, which can be observed in the oscillations of Figs. 8(a) and 8(b), can cause the larger displacements shown in the phase diagrams of Figs. 11(a) and 11(b). Such displacements can disturb the uniformity of the attractor in the phase space. In similar cases the possible existence of a multifractal must be considered. Thus the introduction of generalized dimensions D_q and generalized entropies K_q and the estimation of the corresponding spectra[17–19] may be useful for a complete check of the Grassberger-Proccacia analysis. Work in this field is still going on.

ACKNOWLEDGMENT

The authors would like to thank Professor J. Spyridelis for useful suggestions and his support.

[1]M. Hanias, A. N. Anagnostopoulos, K. Kambas, and J. Spyridelis, Physica B **160**, 154 (1989).
[2]M. Hanias, A. N. Anagnostopoulos, K. Kambas, and J. Spyridelis, Phys. Rev. B **43**, 4135 (1991).
[3]D. Müller, G. Eulenberger, and G. Hahn, Z. Anorg. Allg. Chem. **398**, 207 (1970).
[4]A. T. Nagat, G. A. Gamal, and S. A. Hussein, Phys. Status Solidi A **120**, K163 (1990).
[5]G. D. Guseinov, G. D. Abdullaev, G. B. Bidzinova, S. M. Seidov, F. M. Ismailov, and M. Z. Pashyayev, Phys. Lett. A **33**, 421 (1970).
[6]A. N. Anagnostopoulos, Physica B **162**, 133 (1990).
[7]Abdel-A.Al, A. Elshajie, M. M. El. Zaidia, and A. A. Ammar, Physica B **154**, 105 (1988).
[8]D. M. Kroll, Phys. Rev. B **9**, 1669 (1974).
[9]U. Rau, W. Clauss, A. Kittel, M. Lehr, M. Bayerbach, J. Parisi, J. Peinke, and R. P. Huebener, Phys. Rev. B **43**, 3 (1991); **43**, 2255 (1991).

[10]Ch. Karakotsou, J. A. Kalomiros, M. P. Hanias, A. N. Anagnostopoulos, and J. Spyridelis, Phys. Rev. B **45**, 11 627 (1992).
[11]P. Grassberger and I. Procaccia, Phys. Rev. A **28**, 2591 (1983).
[12]P. Grassberger and I. Procaccia, Phys. Rev. Lett. **50**, 346 (1983).
[13]D. Ruelle, *Chaotic Evolution and Strange Attractors* (Cambridge University Press, Cambridge, 1989), p. 79 ff.
[14]S. Martin, H. Leber, and W. Martienssen, Phys. Rev. Lett. **53**, 303 (1984).
[15]J. Peinke, D. B. Schmid, B. Rohricht, and J. Parisi, Z. Phys. B **66**, 65 (1987).
[16]M. P. Shaw and N. Yildirim, Adv. Electron. Electron Phys. **60**, 307 (1983).
[17]T. C. Halsey, M. H. Jensen, L. P. Kadanoff, I. Procaccia, and B. I. Shraiman, Phys. Rev. A **33**, 1141 (1986).
[18]J. A. Clazier and A. Libchaber, IEEE Trans. Circ. Syst. **35**, 790 (1988).
[19]M. H. Jensen, L. P. Kadanoff, A. Libchaber, I. Procaccia, and J. Stavans, Phys. Rev. Lett. **55**, 2798 (1985).